RESEARCH ARTICLE

Molecular Docking, MD Simulation, and Antiproliferative Activity of Pyridazine Derivatives

Ritik Panwar[1], Vikash Jakhmola[1*], Supriyo Saha[1], Sunil Jawla[2], Ravinesh Mishra[3]

[1]*Department of Pharmaceutical Chemistry, Uttaranchal Institute of Pharmaceutical Sciences, Uttaranchal University, Dehradun-248001, Uttarakhand, India*
[2]*Geeta Institute of Pharmacy, Geeta University, Panipat, Haryana, India*
[3]*School of Pharmacy and Emerging Sciences, Baddi University of Emerging Sciences & Technology, Baddi, Himachal Pradesh, India*

Received: 4th Mar, 2025; Revised: 11th Apr, 2025; Accepted: 7th Jun, 2025; Available Online: 25th Jun, 2025

ABSTRACT
Pyridazine derivative showed much diversified activity. Previously 77 pyridazine derivatives were synthesized and evaluated the antihypertensive property. Pyridazine derivatives also showed antitumor and antiproliferative behavior. By kept this idea in mind we repurposed those pyridazine derivatives towards antiproliferation using *in silico*, and *in vitro* methods. Molecular docking analysis of pyridazine derivatives against DNA (PDB id: 6BNA) were performed and top4 molecules (R45, R60, R67, R70) were identified based on their docking scores. Then 100 ns MD simulation and MMPBSA analysis of these molecules were performed using GROMACS software. MD simulation data showed good RMSD, radius of gyration, SASA, and hydrogen bond analysis. Pyridazine derivative (R67) showed good simulation behavior with very minimum fluctuation within the receptor. Free binding energy of R67 was (-) 42.683 kJ/mol. R67 showed marked GI_{50} value against MCF7 cell line using sulphorhodamine assay. Among the pyridazine derivatives Among the synthesized molecules 6-([1,1'-biphenyl]-4-yl)-2-(4-([1,1'-biphenyl]-4-yl)-5-thioxo-4,5-dihydro-1H-1,2,4-triazol-3-yl)-4,5-dihydropyridazin-3(2H)-one (R67) showed best antiproliferative activity with *in silico* insights.

Keywords: Pyridazine, Molecular docking, MD Simulation, Antiproliferative.
How to cite this article: Ritik Panwar, Vikash Jakhmola, Supriyo Saha, Sunil Jawla, Ravinesh Mishra. Molecular Docking, MD Simulation, and Antiproliferative Activity of Pyridazine Derivatives. International Journal of Drug Delivery Technology. 2025;15(2):748-56. doi: 10.25258/ijddt.15.2.48
Sourse of support: This study is supported by Division of Research & Innovation, Uttaranchal University, Dehradun, India under the seed money grant reference no UU/DRI/SM/2024-25/018.
Conflict of interest: None

INTRODUCTION

The term "cancer" refers to a broad category of illnesses where aberrant cells proliferate out of control and have the potential to spread to other bodily areas. It is categorized according to the type of cell or tissue from which it originates and can form in nearly any tissue or organ. Through the circulation or lymphatic system, cancer cells can penetrate nearby tissues and spread (metastasize) to other parts of the body.[1] Cancer can be categorized in several ways, including by the type of tissue or organ involved. Carcinoma begins in the epithelial cells, which make up the skin or lining of internal organs. Adenocarcinoma is the cancers of glandular cells (e.g., breast, prostate, and lung cancers). Squamous cell carcinoma develop in squamous cells (thin, flat cells found in the skin or lining of internal organs). Common Carcinomas are lung cancer, breast cancer, colon cancer, and pancreatic cancer.[2] Sarcoma is cancer begin in connective tissues like bone, muscle, fat, cartilage, and blood vessels. Osteosarcoma (bone cancer), liposarcoma (cancer of fat tissue), and leiomyosarcoma (cancer of smooth muscle tissue) are the most common types of sarcoma. Bone marrow and blood are affected by leukemia, a malignancy that causes an excess of aberrant white blood cells. Acute leukemia, which progresses quickly and has a short lifespan if left untreated, and chronic leukemia, which progresses more slowly and has a longer survival time, are common forms of leukemia.[3] The lymphatic system, which includes the spleen, bone marrow, and lymph nodes, is where lymphomas are malignancies. One kind of skin cancer called melanoma arises in melanocytes, which are the cells that make the pigment melanin. It is more aggressive than other forms of skin cancer. Myeloma is cancer of the plasma cells in the bone marrow4. Pyridazine is a heterocyclic organic compound with the chemical formula $C_6H_4N_2$. It is a type of azine compound, which means it contains a six-membered ring with two nitrogen atoms (as part of the aromatic structure) and four carbon atoms. Pyridazine has a structure similar to pyridine, but with an additional nitrogen atom in its ring.[4] A novel pyrimidine-pyridazine derivatives were synthesized upon reaction between cyano pyridazine derivatives with substituted phenyl methyl amine using ullmann acylation reaction. Then all the synthesized molecules were assessed against breast cancer cell lines. Among them, molecule (**1**) showed good activity the breast cancer.[5] Griguolo et al developed olaparib (**2**) with good HER2-negative advanced breast

**Author for Correspondence: jakhmola.1979@gmail.com*

cancer.[6] This drug showed good potency of poly (ADP-ribose) polymerase (PARP) enzyme inhibition with good anti cancer activity. Shaalan et al synthesized novel 3,6-disubstituted pyridazine derivatives and among them (**3**) with good inhibition of NCI-60 cancer cell lines.[7] Elmeligie et al synthesized a new pyridazine derivative (**4**) with good inhibition of colon cancer targeting VEGFR kinase enzyme.[8] Sabt et al synthesized a series of pyridazine derivatives (**5**) and (**6**) showed antitumor activities.[9,10] This manuscript focus on the antiproliferative property of pyridazine derivative using *in vitro* and *in silico* methods.

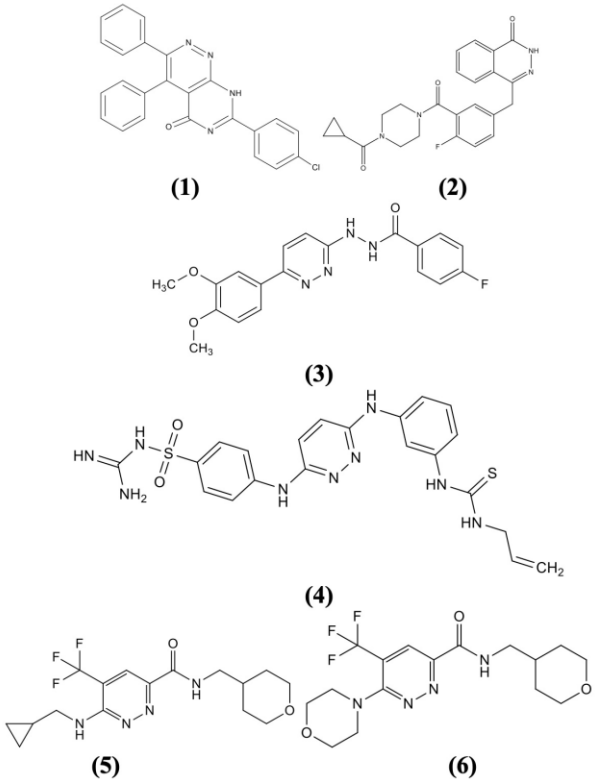

EXPERIMENTAL

Structures of the Molecules

Chemical structures of in house pyridazine molecules were drawn by Avogadro software (Table 1).[11,12]

Molecular Docking Analysis of Pyridazine derivatives with DNA as Antitumor Agent

The binding energy was calculated using a molecular docking research to anticipate ligand-target interactions. Using ligand molecules, the interaction between the ligand and target proteins created an environment that hindered receptor activation in the molecular docking study. The output features showed the potential activity of the ligand molecule. The ligand's structural characteristics upon contact with the receptor were represented in the interactive pose of the ligand molecules within the receptor. The highest to lowest docking conformers were shown in the output energy tabulation.[13] The 6BNA receptor was docked with the 77 pyridazine compounds that were chosen for this study. A member of the deoxyribonucleotide (DNA) class is the 6BNA receptor. There are two chains in the receptor. There existed netrospin (NT) as a complex ligand. Drug Discovery Studio was used to assess the co-crystallized ligand's surrounding residue. The AUTODOCK Vina software was used to conduct the molecular docking investigation, and the Drug Discovery Studio software was used to show the results.[14] The structures of the 77 pyridazine derivatives were optimized and saved in pdbqt format[18]. BIOVIA Discovery Studio Visualizer 4.5 was used to view and analyze the docking data. Center_x = 15.344, center_y = 21.339, center_z = 6.993, size_x = 24, size_y = 24, and size_z = 24 were the grid box sizes of the 6BNA receptor, with exhaustiveness of 8.[15]

Table 1: SMILE Notations of Pyridazine Derivatives

Code of the Molecules	SMILES Notation	Code of the Molecules	SMILES Notation
R1.	O=C1CCC(=NN1CN1CCOCC1)c1ccccc1	R40.	CC(C)Cc1ccc(cc1)C=1CCC(=O)N(Cn2ncnc2)N=1
R2.	O=C1CCC(=NN1CN1CCNCC1)c1ccccc1	R41.	O=C1CCC(=NN1CN1CCOCC1)c1ccc(cc1)c1ccccc1
R3.	O=C1CCC(=NN1CN1CCCCC1)c1ccccc1	R42.	O=C1CCC(=NN1CN1CCNCC1)c1ccc(cc1)c1ccccc1
R4.	CN1CCN(CC1)CN1N=C(CCC1=O)c1ccccc1	R43.	O=C1CCC(=NN1CN1CCCCC1)c1ccc(cc1)c1ccccc1
R5.	O=C1CCC(=NN1CN1c2ccccc2Sc2ccccc12)c1ccccc1	R44.	CN1CCN(CC1)CN1N=C(CCC1=O)c1ccc(cc1)c1ccccc1
R6.	O=C1CCC(=NN1Cn1ccc2ccccc12)c1ccccc1	R45.	O=C1CCC(=NN1CN1c2ccccc2Sc2ccccc12)c1ccc(cc1)c1ccccc1
R7.	O=C1CCC(=NN1CN1CCCC1)c1ccccc1	R46.	O=C1CCC(=NN1Cn1ccc2ccccc12)c1ccc(cc1)c1ccccc1
R8.	O=C1CCC(=NN1Cn1ncnc1)c1ccccc1	R47.	O=C1CCC(=NN1CN1CCCC1)c1ccc(cc1)c1ccccc1
R9.	Cc1ccc(cc1)C1=NN(CN2CCOCC2)C(=O)CC1	R48.	O=C1CCC(=NN1Cn1ncnc1)c1ccc(cc1)c1ccccc1
R10.	Cc1ccc(cc1)C=1CCC(=O)N(CN2CCNCC2)N=1	R49.	Clc1ccc(cc1)C1=NN(CN2CCOCC2)C(=O)CC1
R11.	Cc1ccc(cc1)C=1CCC(=O)N(CN2CCCCC	R50.	Clc1ccc(cc1)C=1CCC(=O)N(CN2CCNCC2)

Table 1: SMILE Notations of Pyridazine Derivatives

Code of the Molecules	SMILES Notation	Code of the Molecules	SMILES Notation
	2)N=1		N=1
R12.	Cc1ccc(cc1)C=1CCC(=O)N(CN2CCN(CCC2)N=1	R51.	Clc1ccc(cc1)C=1CCC(=O)N(CN2CCNCC2)N=1
R13.	Cc1ccc(cc1)C=1CCC(=O)N(N=1)CN1c2ccccc2Sc2ccccc12	R52.	Clc1ccc(cc1)C=1CCC(=O)N(CN2CCN(C)CC2)N=1
R14.	Cc1ccc(cc1)C=1CCC(=O)N(Cn2ccc3ccccc23)N=1	R53.	Clc1ccc(cc1)C=1CCC(=O)N(N=1)CN1c2ccccc2Sc2ccccc12
R15.	Cc1ccc(cc1)C=1CCC(=O)N(CN2CCCC2)N=1	R54.	Clc1ccc(cc1)C=1CCC(=O)N(Cn2ccc3ccccc23)N=1
R16.	Cc1ccc(cc1)C=1CCC(=O)N(Cn2ncnc2)N=1	R55.	Clc1ccc(cc1)C=1CCC(=O)N(CN2CCCC2)N=1
R17.	COc1ccc(cc1)C1=NN(CN2CCOCC2)C(=O)CC1	R56.	Clc1ccc(cc1)C=1CCC(=O)N(Cn2ncnc2)N=1
R18.	COc1ccc(cc1)C=1CCC(=O)N(CN2CCNCC2)N=1	R57.	O=C1CCC(=NN1C1=NNC(=S)N1c1ccc(cc1)c1ccccc1)c1ccccc1
R19.	COc1ccc(cc1)C=1CCC(=O)N(CN2CCCCC2)N=1	R58.	Clc1ccc(cc1)c1ccc(cc1)N1C(=S)NN=C1N1N=C(CCC1=O)c1ccccc1
R20.	COc1ccc(cc1)C=1CCC(=O)N(CN2CCN(C)CC2)N=1	R59.	Cc1ccc(cc1)C=1CCC(=O)N(N=1)C1=NNC(=S)N1c1ccc(cc1)c1ccccc1
R21.	COc1ccc(cc1)C=1CCC(=O)N(N=1)CN1c2ccccc2Sc2ccccc12	R60.	Clc1ccc(cc1)c1ccc(cc1)N1C(=S)NN=C1N1N=C(CCC1=O)c1ccc(C)cc1
R22.	COc1ccc(cc1)C=1CCC(=O)N(Cn2ccc3ccccc23)N=1	R61.	COc1ccc(cc1)C=1CCC(=O)N(N=1)C1=NNC(=S)N1c1ccc(cc1)c1ccccc1
R23.	COc1ccc(cc1)C=1CCC(=O)N(CN2CCCC2)N=1	R62.	Clc1ccc(cc1)c1ccc(cc1)N1C(=S)NN=C1N1N=C(CCC1=O)c1ccc(OC)cc1

Table 1: SMILE Notations of Pyridazine Derivatives

Code of the Molecules	SMILES Notation	Code of the Molecules	SMILES Notation
R24.	COc1ccc(cc1)C=1CCC(=O)N(Cn2ncnc2)N=1	R63.	CCc1ccc(cc1)C=1CCC(=O)N(N=1)C1=NNC(=S)N1c1ccc(cc1)c1ccccc1
R25.	CCc1ccc(cc1)C1=NN(CN2CCOCC2)C(=O)CC1	R64.	Clc1ccc(cc1)c1ccc(cc1)N1C(=S)NN=C1N1N=C(CCC1=O)c1ccc(CC)cc1
R26.	CCc1ccc(cc1)C=1CCC(=O)N(CN2CCNCC2)N=1	R65.	CC(C)Cc1ccc(cc1)C=1CCC(=O)N(N=1)C1=NNC(=S)N1c1ccc(cc1)c1ccccc1
R27.	CCc1ccc(cc1)C=1CCC(=O)N(CN2CCCCC2)N=1	R66.	CC(C)Cc1ccc(cc1)C=1CCC(=O)N(N=1)C1=NNC(=S)N1c1ccc(cc1)c1ccc(Cl)cc1
R28.	CCc1ccc(cc1)C=1CCC(=O)N(CN2CCN(C)CC2)N=1	R67.	O=C1CCC(=NN1C1=NNC(=S)N1c1ccc(cc1)c1ccccc1)c1ccc(cc1)c1ccccc1
R29.	CCc1ccc(cc1)C=1CCC(=O)N(N=1)CN1c2ccccc2Sc2ccccc12	R68.	Clc1ccc(cc1)c1ccc(cc1)N1C(=S)NN=C1N1N=C(CCC1=O)c1ccc(cc1)c1ccccc1
R30.	CCc1ccc(cc1)C=1CCC(=O)N(Cn2ccc3ccccc23)N=1	R69.	Clc1ccc(cc1)C=1CCC(=O)N(N=1)C1=NNC(=S)N1c1ccc(cc1)c1ccccc1
R31.	CCc1ccc(cc1)C=1CCC(=O)N(CN2CCCC2)N=1	R70.	Clc1ccc(cc1)c1ccc(cc1)N1C(=S)NN=C1N1N=C(CCC1=O)c1ccc(Cl)cc1
R32.	CCc1ccc(cc1)C=1CCC(=O)N(Cn2ncnc2)N=1	R71.	N=C1NCN2N=C(CCC2=N1)c1ccccc1
R33.	CC(C)Cc1ccc(cc1)C1=NN(CN2CCOCC2)C(=O)CC1	R72.	Cc1ccc(cc1)C=1CCC2=NC(=N)NCN2N=1
R34.	CC(C)Cc1ccc(cc1)C=1CCC(=O)N(CN2CCNCC2)N=1	R73.	COc1ccc(cc1)C=1CCC2=NC(=N)NCN2N=1
R35.	CC(C)Cc1ccc(	R74.	CCc1ccc(cc1)C

Table 1: SMILE Notations of Pyridazine Derivatives

Code of the Molecules	SMILES Notation	Code of the Molecules	SMILES Notation
	cc1)C=1CCC(=O)N(CN2CCCCC2)N=1		=1CCC2=NC(=N)NCN2N=1
R36.	CC(C)Cc1ccc(cc1)C=1CCC(=O)N(CN2CCN(C)CC2)N=1	R75.	CC(C)Cc1ccc(cc1)C=1CCC2=NC(=N)NCN2N=1
R37.	CC(C)Cc1ccc(cc1)C=1CCC(=O)N(N=1)CN1c2ccccc2Sc2ccccc12	R76.	N=C1NCN2N=C(CCC2=N1)c1ccc(cc1)c1ccccc1
R38.	CC(C)Cc1ccc(cc1)C=1CCC(=O)N(Cn2ccc3ccccc23)N=1	R77.	Clc1ccc(cc1)C=1CCC2=NC(=N)NCN2N=1

Table 1: SMILE Notations of Pyridazine Derivatives

Code of the Molecules	SMILES Notation	Code of the Molecules	SMILES Notation
R39.	CC(C)Cc1ccc(cc1)C=1CCC(=O)N(CN2CCCC2)N=1		

Molecular dynamic simulation and MMPBSA Analysis

Molecular dynamic simulation data helped to understand the structural atomic level dynamics of the ligand molecules upon interaction with the receptors. In this study, the GROMACS 20.1 software package running on the LINUX UBUNTU platform was used to study the thermodynamic characteristics of the ligand-receptor complex.[16]Molecular dynamic simulation (100 ns) studies were performed with top 4 molecules R45, R60, R67, and R70 with best docking scores against antitumor drug binding DNA 6BNA receptors using CHARMM 36 force field and TIP3P water molecules, and ions.[17] The

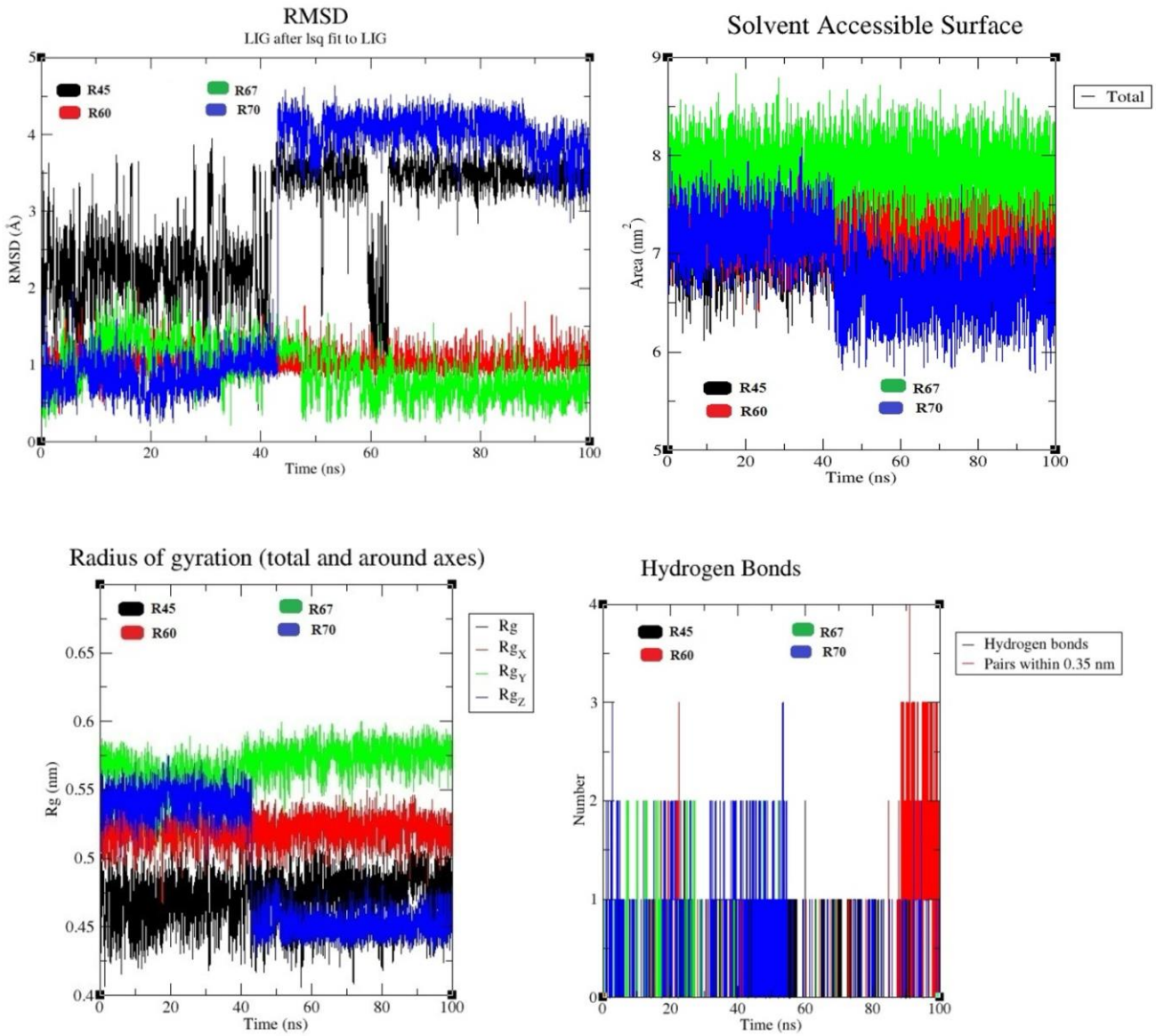

Figure 2: MD Simulation data of best docked pyridazine derivatives interacted with DNA

trajectories of the MD simulation were studied using GROMACS software package. Qtgrace software was used to identify the graphical representation of simulation trajectories. The free binding energies of the complexes were determined by molecular mechanics poisson-boltzmann surface area (MMPBSA) analysis.[18,19]

Antiproliferative Assay of Pyridazine Derivatives against Breast Cancer Cell line

The sulphorodamine B assay was used to evaluate the produced compounds' antiproliferative efficacy against the MCF-7 breast cancer cell line.

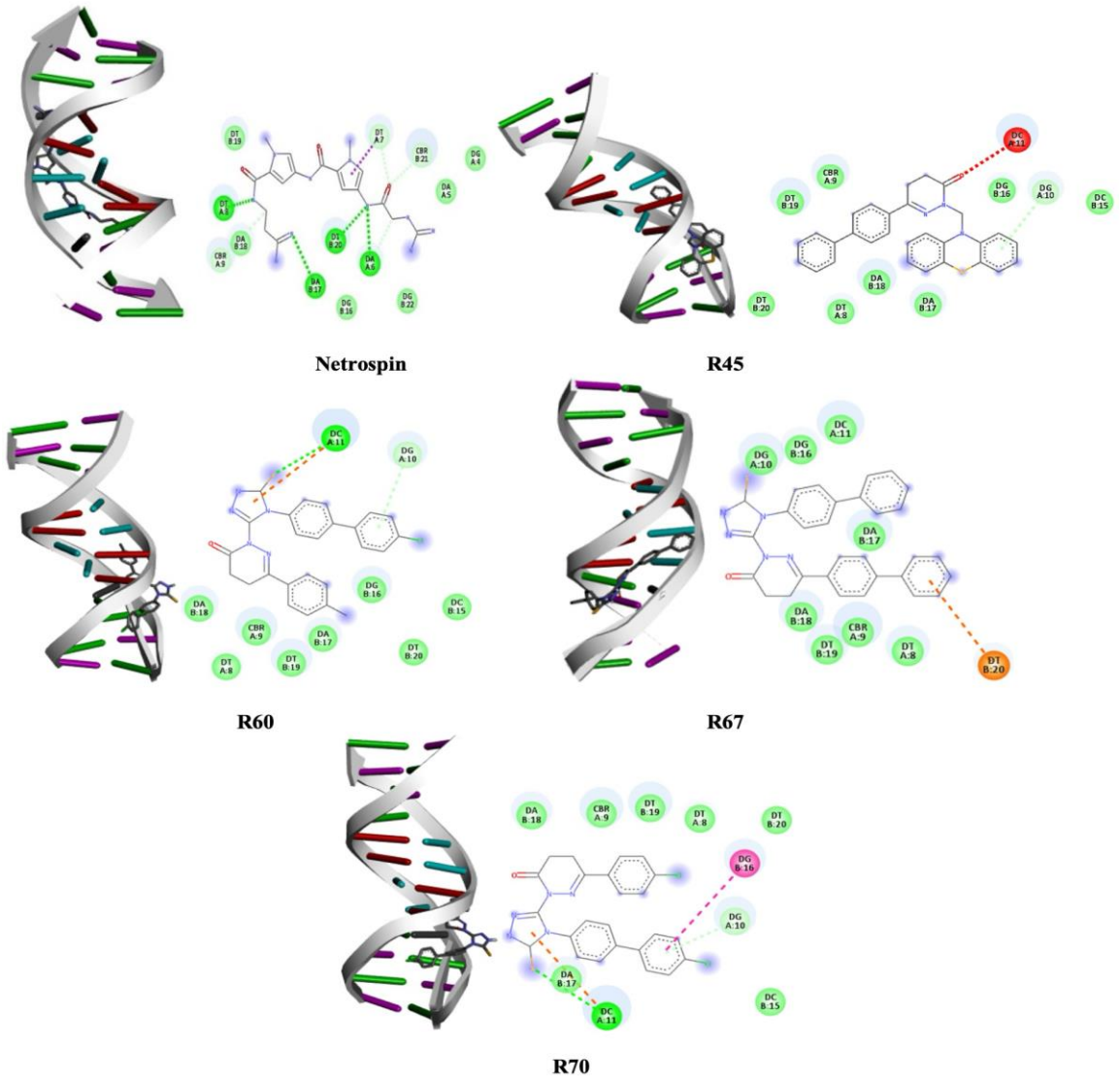

Figure 1: Best docked pyridazine derivatives (R45, R60, R67, R70) interacted with DNA

Table 2: Molecular docking analysis data of Pyridazine derivatives with DNA

SN.	Code of the Molecules	Dock Score (kcal/mol)	Interacting residues
1.	R1	-7.3	DT8a, DA17a, CBR9a, DA18b, DT19b, DC11b, DG10b, DG16b, DG12b.
2.	R2	-7.3	DT8a, DT19b, DA17a, DG10b, DG16b. CBR9b, DA18b, DC11b.
3.	R3	-7.4	DT8a. DA18a, DA17a, DG16b, DG10b, DT19b, DC11b, CBR9b.
4.	R4	-7.4	DA6a, DA5b, DG4b, DG22c, DC3b, DG2b, DG24b, DC23b.
5.	R5	-8.4	DA17a, DG16b, DA18a, DG10b, CBR9a, DT19b
6.	R6	-7.6	CBR9a, DC11b, DA18b, DG10b, DG16b, DA17a, DC15b, DG14b.
7.	R7	-7.3	DA17a, DG16b, DA18a, DG10b, CBR9a, DT19b, DT8b, DT7b, DT20b.
8.	R8	-7.0	DG16a, DG10b, DA17a, DG14a, DC11b, DA18a, CBR9a.
-9.	R9	-8.0	DG22a, DA5a, DT20c, DC3b, DA6b, DC23b, DT78b.
10.	R10	-7.6	DA5a, DC23b, DA6b, DT7b, DG4b, DT20c, DG22c, DC3b.
11.	R11	-8.1	DG22c, DT20c, DG4b, DA5b, DC3b, DC23b, DA6b, DT7b.

Table 2: Molecular docking analysis data of Pyridazine derivatives with DNA

SN.	Code of the Molecules	Dock Score (kcal/mol)	Interacting residues
12.	R12	-7.6	DT19b, CBR9a, DT20b, DT8b, DT7b, DA18b, DG16b, DA17b, DG10b.
13.	R13	-8.9	DT20c, DG22c, DA5b, DG4b, DA6c, DC23c, DT7b.
14.	R14	-8.1	DT19b, DG16b, DG14b, DC15b, DG10a, DC11b, DA17b, DA18b, DT8b, CBR9b.
15.	R15	-7.2	DA18a, DA17a, CBR9b, DG16b, DG10b, DC15b, DG14b, DC11b.
16.	R16	-7.8	DG10b, DG16a, DT19b, DT7b, DT20b, DT8b, DA17a, DA18a.
17.	R17	-7.5	DG16a, DC15b, DG14b, DA18a, DC11a, DT8a, CBR9a, DT19b.
18.	R18	-7.8	DA5a, DG4a, DC3b, DT20c, DG22c, DA6b, DC23a, DT7b.
19.	R19	-7.5	DA18c, DT8a, DT19b, DA17a, DG10b, DG16b, CBR9b, DC11b.
20.	R20	-7.6	DA18b, DG10b, DC11b, DG16a, DT19b, CBR9b, DT8b, DA17a.
21.	R21	-9.0	DA18c, CBR9b, DT19b, DT8a, DA17b, DG12b, DG10a, DC11b, DC15b, DC15b.
22.	R22	-8.4	DA18a, DC11b, DG14b, DC15b, FG16a, DA17b, DT8b, DT19b, CBR9b.
23.	R23	-7.2	DT7b, DG22a, DT20c, DC3b, DG4b, DA5b, DC23b, DA6b.
24.	R24	-7.9	DA17b, DG16a, DG10b, DA18a, CBR9b, DT8b, DT20b, DT19b, DT7a.
25.	R25	-7.6	DA18a, CBR9b, DC11b, DT19a, DT8a, DG16a, DA17b, DG10a, DG14b, DC15b.
26.	R26	-7.5	CBR9a, DA18a, DT19b, DA6c, DT7c, DT8b, DT20c.
27.	R27	-7.1	DC11a, DG16a, DG10b, DT19b, DA17a, CBR9b, DA18c.
28.	R28	-7.5	CBR9a, DA18a, DA17a, DG10a, DC11a, DT19b.
29.	R29	-8.8	DG10a, DT8c, CBR9b, DA18c, DT19b.
30.	R30	-8.1	DG10a, CBR9b, DA17b, DA18b.
31.	R31	-7.2	DC11a, DG16a, DA17a, DG10b.
32.	R32	-7.4	DT20c, DG22c, DG4b.
33.	R33	-7.9	DT20c, DA6b, DC23b, DA5a, DG22c, DG4b.
34.	R34	-7.8	DA5a, DT20c, DG22c.
35.	R35	-7.5	DG10b, DG16a, DC15a, DG12b, DC11b.
36.	R36	-7.7	DT20c, DG22a, DC23b, DA5b, DC3b, DC7b.
37.	R37	-8.5	DG22a, DA5b, DG24b, DG4b, DT20b.
38.	R38	-8.6	DG10a, DC15b, DG16b, CBR9b, DA18b.
39.	R39	-7.2	DA17a, DA18a, CBR9b, DG10b, DC11b.
40.	R40	-7.4	DG4a, DG22a, DA5b, DA6a, DT20c.
41.	R41	-8.6	DA18a, CBR9a, DG10b, DA17a, DG16b.
42.	R42	-8.6	DA17a, DG16a, DG10a, DC11a, DA18b, DT8b.
43.	R43	-8.7	DT19c, DG10a, DC11a, DA17b.
44.	R44	-9.0	CBR9a, DG16b, DA17b, DG10b, DT8b.
45.	R45	-10.1	DG10a, DC15b, DA17b, CBR9b.
46.	R46	-9.2	DG10a, DA17b, DA18b, CBR9b.
47.	R47	-8.4	DA5a, DG22c, DT20c, DC3b, DA6b.
48.	R48	-8.4	DG10a, DC11a, DT19c, DG16a.
49.	R49	-7.5	DG16a, DA17b, CBR9a, DA18a, DT8a, DC15b.
50.	R50	-7.5	CBR9a, DA17b, DG16b, DA18b.
51.	R51	-7.4	DG10a, DC11b, DG16a, DA18b, CBR9b, DC15b.
52.	R52	-7.8	DA17a, DA18a, DTA19a, CBR9b, DC11b.
53.	R53	-8.4	DG22a, DA5b, DC23b, DG4b, DG2b.
54.	R54	-8.1	DG10a, DC11b, DG14b, CBR9b, DT8b.
55.	R55	-7.2	DA18a, DA17a, CBR9b, DG10b, DC11b.
56.	R56	-7.9	DG16a, DA18a, DA17a, CBR9b, DT19b.
57.	R57	-9.4	DG10b, DC11b, DA17b, DA18b, CBR9b, DT19b.
58.	R58	-9.8	DC11a, DG10b, DA18b, CBR9b, DG16b.
59.	R59	-7.5	DG10c, DT20b, DT19b, DT8b, DG16b.
60.	R60	-10.1	DC11a,c, DG10b, DG16b,CBR9b.
61.	R61	-7.7	DT20b, DT19b, CBR9b, DT8b, DA18b, DG16b, DG10.
62.	R62	-9.9	DC11a,c, DA18b, CBR9b, DA17b, DT8b, DG16b, DG10b, DC15b.
63.	R63	-7.5	DC11a, DG10b, DT19c, DT20b, DA18b, CBR9b, DA17b.
64.	R64	-9.9	DC11a, DG10a, DA18b, CBR9b, DT20b, DC15b.

Table 2: Molecular docking analysis data of Pyridazine derivatives with DNA

SN.	Code of the Molecules	Dock Score (kcal/mol)	Interacting residues
65.	R65	-7.8	DG10c, DT20a, DA17c, DT8b, DT19b, CBR9b, DG16b, DC11b.
66.	R66	-7.7	CBR9a, DA18c, DT19b, DG16a, DG10b, DA17b, DC11b.
67.	R67	-10.4	DG10b, DG16b, DC11b, DA17b, DA18b, CBR9b, DT8b, DT20c.
68.	R68	-9.6	DT7c, DG24c, DT20b, CBR9b, DT8b, DT19b, DG4b, DA5b.
69.	R69	-7.4	DT19b, DT20b, DC11b, DG10b, DA18b, CBR9b, DG16b.
70.	R70	-10.1	DC11a, DA17b, DC15b, DG10a, DG16c, DT20b, DT8b.
71.	R71	-6.6	DA18a, DA17a, DC11b, DG16b, DG10a.
72.	R72	-7.7	DG10a, CBR9a, DA18a, DA17a, DG16b, DG14b, DC15b.
73.	R73	-7.8	DC11a, DG16a, DA17b, DC15b, DT19b, CBR9b.
74.	R74	-7.9	DC15a, DC11a, DG16a, DG12b, CBR9b.
75.	R75	-7.7	DT8a, DA18a, CBR9b, DT19b, DG10b, DC11b.
76.	R76	-8.7	DA6a, DG22a, DT20c, DT7b, DA5c, DG4b, DC3b.
77.	R77	-7.8	CBR9a, DA18a, DA17a, DG16b, DG10a, DC15b, DG14b, DC11b.

a: Hydrogen bond,b:Van der wal interactions, c:Pi bond

Table 3: Antiproliferative activity data of Pyridazine derivatives on MCF-7

SN	Code of Pyridazine Derivatives	LC50	TGI	GI_{50} (μM)
1.	R45	>80	>80	20.1
2.	R60	>80	>80	29.7
3.	R67	>80	>80	11.6
4.	R70	>80	>80	31.5
5.	Adriamycin	52.6	16.8	-48.4

First, trichloroacetic acid was used to establish the culture, and then sulforhodamine B was used for staining. After that, 10 mM unbuffered tris base [tris hydroxymethyl] aminomethane was used to remove the protein-linked dye in order to measure optical density.[20]

An acetic acid solution was used to wash the protein-unbound dye. The Lowry and Bradford test protocols served as the basis for the SRB assay. With 1000 cells, the signal to noise ratio at 564 nm was 1.5. In order to measure cell toxicity, this method demonstrated a highly desired automated drug screening procedure. Static fluorescence cytometry was used to measure SRB fluorescence at 488 nm under laser illumination.[21]

RESULTS AND DISCUSSION

Molecular Docking Analysis Data

DNA was docked with all 77 of pyridazine derivatives (R1–R77) (PDB id: 6BNA).[22] Netrospin engaged in hydrogen bond interactions with DA (A6), DA (B17), DT (A8), and DT (B20) inside the receptor complexed ligand; pi-sigma interactions with DT (A7); and van der Waals contacts with DA (B18), DT (B19), and DG (B16). The 77 pyridazine derivatives' docking scores (R1–R77) fell between -6.6 and -10.4 kcal/mol20. Every molecule was precisely positioned inside the receptor's active site. According to Table 2 and Figure 1, the maximal docking interaction scores for R67, R70, R60, and R45 were -10.4 kcal/mol, -10.1 kcal/mol, -10.1 kcal/mol, and -10.1 kcal/mol, respectively.[24]

MD Simulation and MMPBSA Analysis Data

Average RMSD values of R45, R60, R67, R70 molecules interacted with 6BNA receptor were 2.88 Å, 1.02 Å, 0.91 Å, and 2.66 Å, respectively. RMSD values for R45 and R70 achieved steady value near 70 ns, and 50 ns, respectively. R60 maintain a steady value throughout the simulation time. R67 achieved static value with very minimal fluctuation during simulation. Average SASA values of R45, R60, R67, and R70 molecules interacted with 6BNA receptor were 7.13 nm^2, 7.29 nm^2, 7.87 nm^2, and 6.86 nm^2, respectively. SASA values for R45, R60, and R67 were steady during simulation, and R70 fluctuated during (0-50) ns followed by steady value in the latter 50 ns simulation time.[25] SASA values create positive impact on interaction of ligand molecule with receptor. Average radius of gyration values of R45, R60, R67, and R70 molecules interacted with 6BNA receptor were 0.37 nm, 0.42 nm, 0.45 nm, and 0.41 nm, respectively.[26] Radius of gyration values of R45, R60, and R67 achieved a steady value and R70 achieved a steady value between (40-100) ns. Radius of gyration showed greater stability between ligand and receptor. Hydrogen of R45, R60, R67, and R70 molecules interacted with 6BNA receptor formed good quality hydrogen bonds between ligand and receptor throughout the simulation timeline (Figure 2).[27] MMPBSA analysis of R45, R60, R67, R70 showed that binding energies of -30.656 kJ/mol, -29.503 kJ/mol, and -42.683 kJ/mol, and -27.747 kJ/mol, respectively. Polar solvation energy was negatively impacted on binding energy.[28]

Antiproliferative Analysis Data of Pyridazine Derivatives on Breast Cancer Cell line

In this experiment, (LC_{50}: Lethal Concentration for 50% inhibition), (TGI: Total Growth Inhibition) and (GI_{50}: 50% Growth Inhibition) of the selected pyridazine derivatives (R45, R60, R67, and R70) were determined by taking adriamycin as control. The GI_{50} value of R45, R60, R67, R70 and adriamycin (standard) observed at 20.1 μM, 29.7 μM, 11.6 μM, 31.5 μM, and (-) 48.4 μM, respectively.[29] Among the selected pyridazine derivatives, R67 showed marked GI_{50} value (Table 3).[30]

CONCLUSION

Pyridazine derivatives showed diversified activities. This manuscript mainly focused on the antiproliferative profiling of previously synthesized pyridazine derivatives using sulphorhodamine assay on breast cancer cell line and computationally established their role targeting DNA molecule. Among the synthesized molecules 6-([1,1'-biphenyl]-4-yl)-2-(4-([1,1'-biphenyl]-4-yl)-5-thioxo-4,5-dihydro-1H-1,2,4-triazol-3-yl)-4,5-dihydropyridazin-3(2H)-one (R67) showed best antiproliferative activity with *in silico* background.

REFERENCES

1. Schwartz SM. Epidemiology of Cancer. Clinical Chemistry. 2024; 70: 140-149. doi: 10.1093/clinchem/hvad202
2. Roy PS, Saikia BJ. Cancer and cure: A critical analysis. Indian Journal of Cancer. 2016; 53, 441-442. doi: 10.4103/0019-509X.200658
3. Zhang Q, Wu S. Tertiary lymphoid structures are critical for cancer prognosis and therapeutic response. Frontiers in Immunology. 2023; 13,: 1063711. doi: 10.3389/fimmu.2022.1063711.
4. Medford AJ, Gillani RN, Park BH. Detection of Cancer DNA in Early Stage and Metastatic Breast Cancer Patients. Methods in Molecular Biology. 2018; 1768: 209-227. doi: 10.1007/978-1-4939-7778-9_13.
5. Smith ALM, Whitehall JC, Greaves LC. Mitochondrial DNA mutations in ageing and cancer. Molecular Oncology. 2022; 16: 3276-3294. doi: 10.1002/1878-0261.13291.
6. Benesova L, Belsanova B. Suchanek S, Kopeckova M, Minarikova P, Lipska L, Levy M, Visokai V, Zavoral M, Minarik M. Mutation-based detection and monitoring of cell-free tumor DNA in peripheral blood of cancer patients. Analytical Biochemistry. 2013; 433: 227-34. doi: 10.1016/j.ab.2012.06.018.
7. Griguolo G, Dieci MV, Miglietta F, Guarneri V, Conte P. Olaparib for advanced breast cancer. Future Oncology. 2020; 16: 717-732. doi: 10.2217/fon-2019-0689.
8. Shaalan MM, Osman EEA, Attia YM, Hammam OA, George RF, Naguib BH. Novel 3,6-Disubstituted Pyridazine Derivatives Targeting JNK1 Pathway: Scaffold Hopping and Hybridization-Based Design, Synthesis, Molecular Modeling, and In Vitro and In Vivo Anticancer Evaluation. ACS Omega. 2024; 9: 37310–37329. https://doi.org/10.1021/acsomega.4c05250
9. Elmeligie S, Ahmed EM, Abuel-Maaty SM, Zaitone SA, Mikhail DS. Design and Synthesis of Pyridazine Containing Compounds with Promising Anticancer Activity. Chemical and Pharmaceutical Bulletin. 2017; 65: 236-247. doi: 10.1248/cpb.c16-00532.
10. Sabt A, Eldehna WM, Al-Warhi T, Alotaibi OJ, Elaasser MM, Suliman H, Abdel-Aziz HA. Discovery of 3,6-disubstituted pyridazines as a novel class of anticancer agents targeting cyclin-dependent kinase 2: synthesis, biological evaluation and in silico insights. Journal of Enzyme Inhibition and Medicinal Chemistry. 2020; 35: 1616-1630. doi: 10.1080/14756366.2020.1806259.
11. Varshney M, Mishra R, Ansori ANM, Saha S, Dangwal A, Jakhmola V. In Silico and In Vitro Alpha-amylase Activities of Previously Synthesized Pyridazine Derivatives. Philippines Journal of Science. 2024; 153: 1107–1150.
12. Kawsar SMA, Hossain MA, Saha S, Abdallah EM, Bhat AR, Ahmed S, Jamalis J, Ozeki Y. Nucleoside-Based Drug Target with General Antimicrobial Screening and Specific Computational Studies against SARS-CoV-2 Main Protease. Chemistryselect. 2024; 9: e202304774. https://doi.org/10.1002/slct.202304774
13. Zainul R, Satriawan H, Shalsabilla D. Novel, R. Verawati, A. Putri Lubis, V. Jakhmola, M. Rebezov, S. Syafrizal. S. Ahmed, M. Lakshmi, Analgesic Serotonin from Banana Fruit (Musa paradisiaca) on Serotonin 1 b (5-HT1b) Receptor Protein In Silico. Journal of Applied Organometallic Chemistry. 2024; 4: 88-99. https://doi.org/10.48309/jaoc.2024.443746.1166
14. Kayes MR, Saha S, Alanazi MM, Ozeki Y, Pal D, Hadda TB, Legssyer A, Kawsar SMA. Macromolecules: Synthesis, antimicrobial, POM analysis and computational approaches of some glucoside derivatives bearing acyl moieties. Saudi Pharmaceutical Journal. 2023; 31: 101804. doi: 10.1016/j.jsps.2023.101804.
15. Akter S, Alhatlani BY, Abdallah EM, Saha S, Ferdous J, Hossain ME, Ali F, Kawsar SMA. Exploring Cinnamoyl-Substituted Mannopyranosides: Synthesis, Evaluation of Antimicrobial Properties, and Molecular Docking Studies Targeting H5N1 Influenza A Virus. Molecules. 2023; 28; 8001. doi: 10.3390/molecules28248001.
16. Prinsa, Saha S, Bulbul MZH, Ozeki Y, Alamri MA, Kawsar SMA. Flavonoids as potential KRAS inhibitors: DFT, molecular docking, molecular dynamics simulation and ADMET analyses. Journal of Asian Natural Products Research. 2024; 26: 955-992. doi: 10.1080/10286020.2024.2343821.
17. Isa AS, Uzairu A, Umar UM, Ibrahim MT, Umar AB, Tabti K, Mohammed AM. In silico exploration of novel EGFR-targeting compounds: integrative molecular modeling, docking, pharmacokinetics, and MD simulations for advancing anti-cervical cancer therapeutics. Scientific Reports. 2025; 15: 7334. https://doi.org/10.1038/s41598-025-91135-4
18. Munir I, Batool Z, Khan F, Hussain J, Khan A, Mali SN, Radhakrishnan VV, Almutairi TM, Al-Harrasi A, Shafiq Z, Mathew B, Akram MS. Design, synthesis, in vitro, and in silico studies of novel isatin-hybrid hydrazones as potential triple negative breast cancer agents. RSC Advances. 2025; 15: 948. DOI: 10.1039/d4ra07650h
19. Mushtaq A, Naseer MM. Novel s-triazine derivatives

as potential anticancer agents: Synthesis, DFT, DNA binding, molecular docking, MD simulation and in silico ADMET profiling. Journal of Molecular Structure. 2025; 1322: 140558. https://doi.org/10.1016/j.molstruc.2024.140558

20. Drew Y, Zenke FT, Curtin NJ. DNA damage response inhibitors in cancer therapy: lessons from the past, current status and future implications. Nature Reviews Drug Discovery. 2025; 24: 19-39. https://doi.org/10.1038/s41573-024-01060-w
21. Ashadul Md Sk, Hemalatha K, Matada GSP, Pal R, Manjushree BV, Mounika S, Haripriya E, Viji MP, Anjan D. Current developments in PI3K-based anticancer agents: Designing strategies, biological activity, selectivity, structure-activity correlation, and docking insight. Bioorganic Chemistry. 2025; 154: 108011. https://doi.org/10.1016/j.bioorg.2024.108011
22. Altwaijry NA, Omar MA, Mohamed HS, Mounier MM, Afifi AH, Srour AM. Design, synthesis, molecular docking and anticancer activity of benzothiazolecarbohydrazide–sulfonate conjugates: insights into ROS-induced DNA damage and tubulin polymerization inhibition. RSC Advances. 2025; 15: 5895. DOI: 10.1039/d4ra07810a
23. Lu JX, Lan HR, Zeng D, Song JY, Hao YT, Xing AP, Shen A, Yuan J. Design, synthesis, anticancer activity and molecular docking of quinoline-based dihydrazone derivatives. RSC Advances. 2025; 15: 231-243. DOI: 10.1039/D4RA06954D
24. Omidkhah N, Chamani J, Fatemi F, Hadizadeh F, Lavaee P, Ghodsi R. Synthesis, cytotoxicity, docking, MD simulation, drug-likeness, ADMET prediction and multi spectroscopic studies of some novel quinoline-4-carboxamide derivatives as DNA intercalating and anticancer agents. Journal of Molecular Structure. 2025; 1322: 140334.
25. Alrouji M, Yasmin S, Alshammari MS, Alhumaydhi FA, Sharaf SE, Shahwan M, Shamsi A. Virtual screening and molecular dynamics simulations identify repurposed drugs as potent inhibitors of Histone deacetylase 1: Implication in cancer therapeutics. PLoS ONE. 2025; 20: e0316343. https://doi.org/10.1371/journal.pone.0316343
26. Zhang S, Wu N, Geng Y, Guan L, Niu MM, Li J, Zhu L. A combinatorial screening protocol for identifying novel and highly potent dual-target inhibitor of BRD4 and STAT3 for kidney cancer therapy. Frontiers in Pharmacology. 2025; 16: 1560559. doi: 10.3389/fphar.2025.1560559
27. Wang H, Wu J, Fang Y, Li Q. MD Simulation Reveals a Trimerization-Enhanced Interaction of CD137L with CD137. International Journal of Molecular Sciences. 2025; 26: 1903. https://doi.org/10.3390/ijms26051903
28. Mahapatra M, Das RP, Pakeeraiah K, Mal S, Panda PK, Mekap SK, Paidesetty SK. In Silico Investigation and MD Simulation Approaches of Newly Designed Quercetin-Imidazole Analogs for Anticancer and Antifungal Efficacy. Chemistryselect. 2025; 10: e202404121. https://doi.org/10.1002/slct.202404121
29. El-Ajaily MM, Sarangi AK, Mohapatra RK, Hassan SS, Eldaghare RN, Mohapatra PK, Raval MK, Das D, Mahal A, Cipurkovic A, Al-Noor TH. Transition Metal Complexes of (E)-2((2-hydroxybenzylidene) amino-3-mercaptopropanoic acid: XRD, Anticancer, Molecular modeling and Molecular Docking Studies. Chemistryselect. 2019; 4; 9999-10005. https://doi.org/10.1002/slct.201902306
30. Vaarla K, Karnewar S, Panuganti D, Peddi SR, Vedula RR, Manga V, Kotamraju S. 3-(2-(5-Amino-3-aryl-1H-pyrazol-1-yl) thiazol-4-yl)-2H-chromen-2-ones as Potential Anticancer Agents: Synthesis, Anticancer Activity Evaluation and Molecular Docking Studies. . Chemistryselect. 2019; 4: 4324-4330. https://doi.org/10.1002/slct.201902306